2024 IEEE International Conference on Robotics and Automation (ICRA 2024)
May 13-17, 2024. Yokohama, Japan

Design of a Knee-joint Exoskeleton to Reduce Misalignment in Both the Sagittal and Coronal Planes

Shubhranil Sengupta[1] and Jee-Hwan Ryu[2]

***Abstract*— Many individuals experience knee dysfunctions attributed to the natural aging process and degenerative conditions. To aid individuals in regaining knee functionality, supportive exoskeletons were designed to be affixed to both the shin and thigh. However, a common issue encountered in knee exoskeletons involves the misalignment of joints between the exoskeleton and the user, resulting in discomfort and potential injuries. To reduce misalignment with the knee joint, it is essential for the thigh and shin harnesses of the exoskeleton to replicate the natural trajectories of the knee. However, achieving this is a complex task due to the shifting center of rotation of the knee in both the Sagittal and Coronal planes. Previous knee exoskeletons primarily focus on aligning the joint in the Sagittal plane, neglecting alignment in the other dimension due to inherent design constraints. For the first time, this study introduces a knee-joint exoskeleton capable of conforming to the natural movement of the knee in both the Sagittal and Coronal planes, with the aim of minimizing joint misalignment without the use of inherently soft materials. A spherical scissor linkage mechanism (SSLM) was utilized in conjunction with a customized guide rail to adjust the center of rotation of the SSLM. This configuration facilitates knee flexion/extension while accommodating the knee joint's center of rotation in both the Sagittal and Coronal planes. The experimental outcomes demonstrated a substantial reduction in misalignment with the knee when compared to a commercial knee-support brace with a one-degree-of-freedom revolute joint.**

Fig. 1: Lower-limb exoskeleton with the proposed knee-joint mechanism to reduce joint misalignment. A Spherical Scissor Linkage Mechanism is used in the shin harness for knee flexion and extension, as shown by the green arrow. A customized, guiding rail is used at the thigh harness to constrain the shin harness's motion, recreating the shin's natural trajectory.

I. Introduction

The human knee joint plays a vital role in carrying out daily chores, such as standing, walking, and stair-climbing. While performing these activities, the knee joint must support substantial stress [1], making it prone to injuries. A large number of patients suffer from knee impairment and pain due to aging, and diseases such as post-polio and spinal cord injuries [2], which severely affect their quality of life [3]. Therefore, wearable devices called exoskeletons have been developed, that provide assistive torques at the lower limbs, to help patients restore the functionalities of their knees.

To design a safe and effective exoskeleton for the knee, several issues such as kinematic alignment, joint range of motion, and torque-generation capacity, must be addressed [4]. A general knee-exoskeleton design consists of two rigid links, one for the thigh and the other for the shin, connected by a joint mechanism [5]. The joint mechanism affects the relative motion of one link with respect to the other. These links are strapped around the user's thigh and shin by using harnesses. When the exoskeleton provides assistive torques, the links are actively displaced, which forces the attached thigh and shin to follow. In the desired scenario, the knee-exoskeleton joint constrains the thigh link and shin link along the natural motion trajectory of the thigh and the shin. If this is not achieved, the exoskeleton and the knee move in different directions, resulting in undesired forces being applied to the user's body [6]. This phenomenon is called joint misalignment, which must be minimized to prevent injury and user discomfort [7]. However, designing a suitable knee-joint mechanism to reduce misalignment is challenging due to the knee's complex anatomy [8]. The knee joint has two rotational degrees-of-freedom (DOFs) and is considered a condyloid joint [9]. This means the irregular shape of the condyles changes the knee's center of rotation (COR) non-uniformly along the Sagittal and Coronal planes [10], [11]. Thus, it is difficult to reproduce the natural motion of the thigh and the shin, by single DOF knee-joints with a fixed COR [12], [13], [14].

Past works have proposed various methods to reduce misalignment between the exoskeleton and the knee. Researchers have proposed joint mechanisms that operated parallel to the Sagittal plane, and aligned CORs of the exoskeleton and

This work was supported in part by the Agency for Defense Development under Grant 21-CM-GU-04 funded by the Ministry of National Defense (MND, Korea) and in part by the National Research Foundation of Korea under Grant NRF-2020R1A2C200416914.

[1]The Robotics Program, KAIST, Daejeon, South Korea. Email:shubhranil2016@kaist.ac.kr

[2]Department of Civil and Environmental Engineering, KAIST, Daejeon, South Korea. Corresponding email:jhryu@kaist.ac.kr

the knee mostly along the Sagittal plane [15], [16], [17]. However, the knee's workspace restricted these mechanisms from operating along the Coronal plane, and joint alignment between the knee and these exoskeletons could not be achieved in all three axes. To solve this, soft exoskeletons were developed that passively align and comply with joints, by eliminating rigid structures [18], [19]. However, the soft harnesses cannot support the high-force transmission that the knee requires due to a lack of structural rigidity. Furthermore, the lack of axial rigidity in the harness cannot support the tendons that are used for actuation [20]. This causes the tendons to collapse into the knee's workspace, limiting the user's range of motion.

This article introduces a novel knee-joint exoskeleton that aims to decrease joint misalignment by aligning with the natural trajectory of the knee in both the Sagittal and Coronal planes. As depicted in Figure 1, the proposed joint incorporates a Spherical Scissor Linkage Mechanism (SSLM) [21], enabling knee flexion and extension. Additionally, a rigid guiding rail is employed, specifically designed to adjust the center of rotation of the SSLM to align with the changing COR of the knee in all three axes. Experimental outcomes confirmed a significant reduction in joint misalignment, compared to a commercial knee-support brace with a single degree-of-freedom (DOF) revolute joint. This is the first attempt, to the best of the authors' knowledge, to align the knee joint in all three dimensions without the use of inherently soft materials. Empirical evidence affirmed the exoskeleton's dual characteristics of axial robustness and knee joint adaptability, eliminating the need for soft materials.

II. Background

A. Planar Scissor Linkage Mechanism

The scissor linkage mechanism consists of two or more interconnected rigid links, resembling a pair of scissors. It exhibits compliance only in its direction of motion, and has mechanical constraints to maintain structural rigidity in other directions. Because of this characteristic, it is widely used in heavy lifting and support applications, such as vehicle jacks, lifting tables, and automotive equipment. As depicted in Fig. 2, each rigid link can be interconnected to other links strategically to achieve an extension and retraction mechanism, from the combined effect of the rotational motion of individual links.

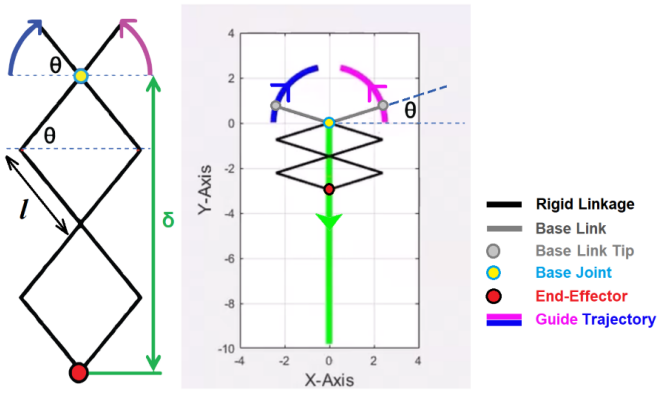

Fig. 2: Planar scissor linkage mechanism notations. When the tips of the base links are displaced along the circular guide trajectory by link angle, θ, the end effector extends by δ along the y-axis. The base joint lies on the origin, and the yaw about the base joint is assumed to be constrained.

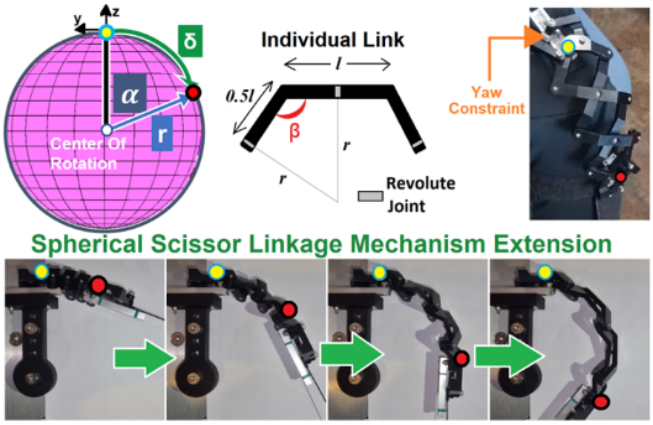

Fig. 3: Notation and working principle of the Spherical Scissor Linkage Mechanism (SSLM). Individual links in the SSLM are bent and have three revolute joints. The bends allow SSLM to achieve a spherical motion. Mechanical yaw constraint limits the SSLM motion to a y-z planar circle.

Fig. 2 illustrates how the scissor mechanism's end-effector motion can be controlled by designing guiding trajectories that constrain the base link tips. The base joint is fixed at the origin and the yaw of the mechanism about the base joint is assumed to be prevented by designing suitable mechanical constraints. The end-effector is defined to be the revolute joint connecting the tips of the end links. By restricting the base link tips to move only along the circular guide trajectory, and the end-effector translates only along the y-axis, as seen in Fig. 2. The angular displacement of the links from the x-axis, referred to as the link angle θ, kinematically determines the end-effector translation, δ as given in (1).

$$\delta = 2nl\sin\theta \tag{1}$$

In (1), l is the link length, and n is the number of pairs of identical links excluding the base links. Link angle θ can be varied to directly control the end-effector displacement δ.

B. Spherical Scissor Linkage Mechanism

The Spherical Scissor Linkage Mechanism (SSLM) is an extended version of the planar scissor linkage mechanism. For the SSLM, the workspace of the base joint and the end-effector spans the surface of a sphere as shown in Fig. 3. The links of the SSLM are symmetrically bent at the two ends by a bending angle, β. The bending angle, and the link length l, affect the radius r of the SSLM's spherical workspace by the kinematic relationship in (2).

$$r = \frac{l * \tan(\frac{\beta}{2})}{2} \tag{2}$$

The SSLM's workspace can be constrained to a y-z planar circle, by adding mechanical components to limit the SSLM's yaw about the base joint. We define the origin of the

y-z plane to lie on the base joint, and the COR lies on the z-axis. Link angle, θ, is defined as the angular displacement of the base link from the x-axis about the base joint, similar to Fig. 2. An increase in θ in the x-y plane causes SSLM extension δ in the y-z plane. During SSLM extension, the angle of rotation, α, can be directly controlled by varying θ, due to the Spherical Law of Cosines [21] as seen in (3).

$$\alpha = n\cos^{-1}(\cos\beta^2 + \sin\beta^2\cos 2\theta) \tag{3}$$

where n is the number of pairs of identical links excluding the base links.

III. Proposed Knee Joint Mechanism

The proposed knee-joint mechanism, depicted in Fig. 4, aims to align the motion of the exoskeleton's thigh and shin harnesses with the natural trajectory of the knee in all three axes. While the mechanism must accommodate the knee's natural motion, it also needs to maintain axial rigidity to support the tendons responsible for joint actuation. This prevents the tendons from collapsing into the knee's workspace and restricting the user's full range of motion. Achieving this requires the Spherical Scissor Linkage Mechanism (SSLM) to maintain a constant moment arm, even under significant axial force.

Initially, the focus is on aligning the thigh and shin harnesses with the knee's natural trajectory. The sole use of the SSLM does not mitigate joint misalignment. When solely employed, the base joint and the end-effector of the SSLM can be attached to the thigh harness and the shin harness, respectively, as illustrated in Fig. 5. For a knee flexion angle of σ, the SSLM must extend by rotation angle α. This condition can be expressed by (4).

$$\alpha = \sigma \tag{4}$$

However, the SSLM possesses a fixed center of rotation (COR). Anchoring the base joint to the thigh harness leads to joint misalignment during knee flexion, since the COR of the knee changes along both the Sagittal and Coronal planes unlike the fixed COR of the SSLM. Instead, the COR of the SSLM can be varied if the tips of the SSLM's base links

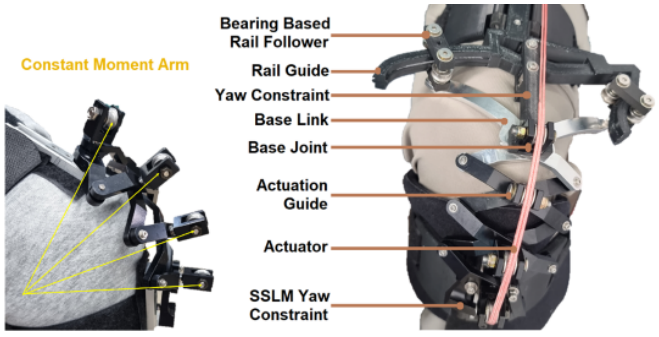

Fig. 4: The proposed knee joint design. The joint is actuated by tendon-based actuators, and the tendon routing is illustrated. The axial rigidity of the Spherical Scissor Linkage Mechanism ensures a constant moment arm, supporting and preventing interference of the tendons with the knee.

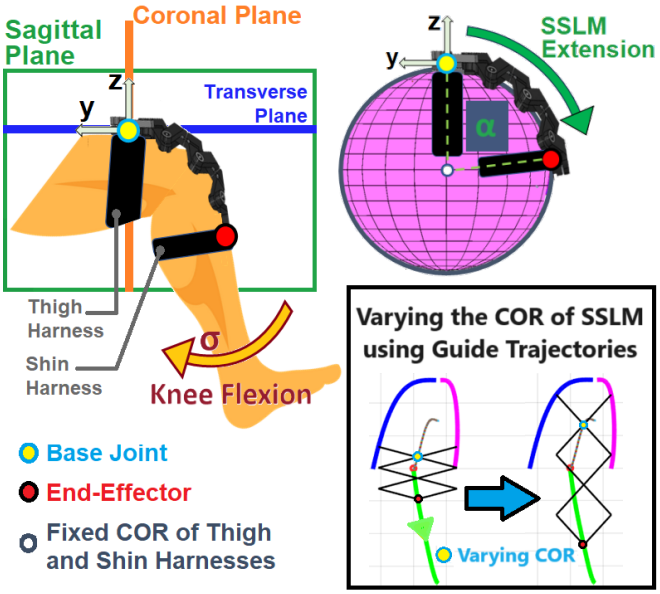

Fig. 5: Usage of the Spherical Scissor Linkage Mechanism (SSLM) as the knee joint. Fixing the SSLM base joint to the thigh harness creates a fixed center of rotation (COR), which causes misalignment with the knee's changing COR during knee flexion. To vary the COR of the SSLM, the tips of the base links can be followed along non-circular guide trajectories.

are moved along rail guides with non circular trajectories, as shown in Fig. 5.

The shape of the rail guide, as observed in Fig. 4, can be configured to ensure alignment of the CORs of the knee and the SSLM at every discrete knee flexion angle, denoted as σ, throughout the entire range of motion. To do so, (3) and (4) are combined to get obtain (5).

$$\sigma = n\cos^{-1}(\cos\beta^2 + \sin\beta^2\cos 2\theta) \tag{5}$$

From (5), it is evident that when both the SSLM and the knee joints are perfectly aligned, there exists a unique base link angle, θ, for every knee flexion angle, σ. To implement

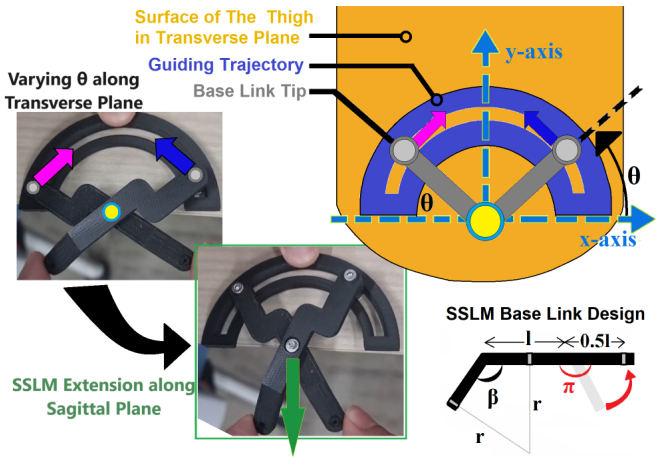

Fig. 6: Modification of the Spherical Scissor Linkage Mechanism's (SSLM's) link design to create a base link. The base link can be used in the Transverse Plane to vary the link angle, θ, to control the end-effector position in the Sagittal Plane. Every θ is mapped onto a corresponding knee flexion angle, σ, when the SSLM and knee's CORs are perfectly aligned.

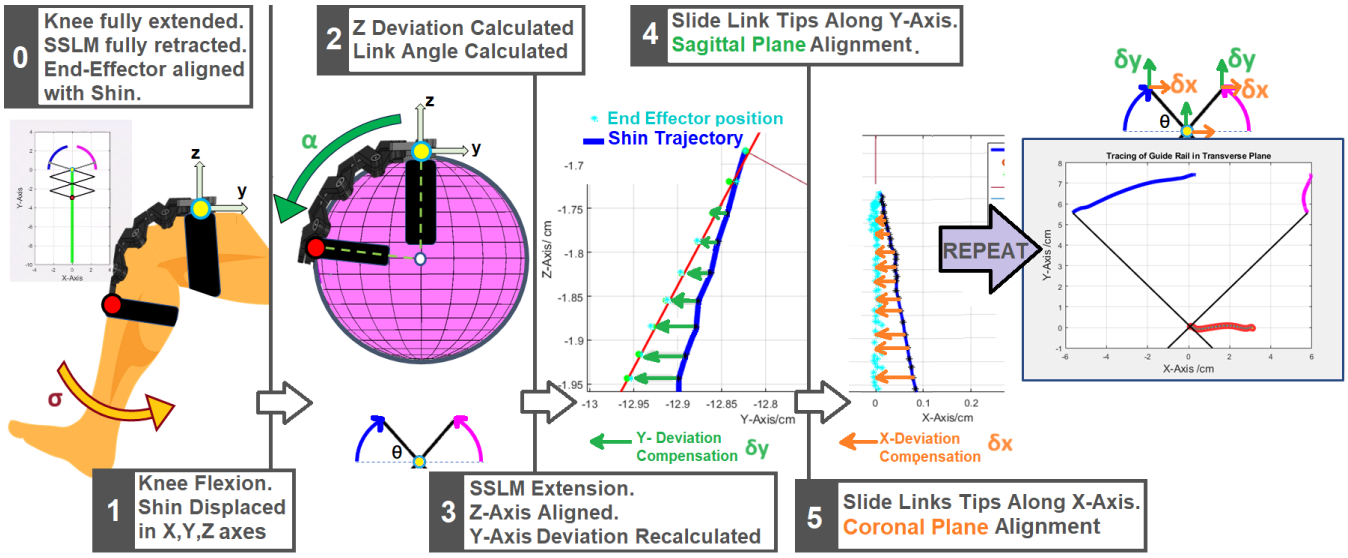

Fig. 7: The iterative process for generating the Transverse guiding trajectory, to reduce misalignment in both the Sagittal and Coronal planes. Actions are performed sequentially to align the SSLM end-effector with each discrete shin-trajectory point, iterating through all data points for the entire motion.

this, the outer surface of the thigh is assumed to lie in the x-y axial Transverse plane, and the shape of the SSLM link is modified to straighten ($\pi = 180°$) one end of a traditional SSLM link to create a base link, as shown in Fig. 6. By varying the tips of the SSLM base links, θ can be adjusted in the transverse plane to control the position of the end-effector in the y-z axial Sagittal plane. We assumed that the base joint incorporates yaw constraints, as shown in Fig. 3, to prevent yaw in the SSLM about the base joint. This ensures that the link angles θ from the x-axis are equal for both base links in Fig. 6.

The next step is an iterative process that allows tracing the shape of the rail guide, illustrated for a single step in Fig. 7. This process is repeated over every discrete knee flexion angle, given that the natural trajectory data of the shin with respect to the thigh are known through accurate tracking methods. Initially, the SSLM is fully retracted and the knee is fully extended. The end-effector lies on the shin, assuming complete alignment. A small amount of knee flexion, σ_1, occurs, causing the shin to slightly displace from the end-effector. The new σ_1 can be calculated from the trajectory tracking data using the method shown in Fig. (9), and using (5), θ_1 can be calculated. Next, the base link angles are set to θ_1, which extends the SSLM and aligns the end-effector and the shin along the z-axial level. The end-effector is still deviated from the shin along the x and y axes by amounts δx and δy. For this new SSLM configuration with a base link angle θ_1, base link tips can be displaced by amounts δx and δy on the Transverse planar thigh, to align the end-effector in the remaining two axes. Alignment is now complete in all three axes for the current knee flexion angle, and this is the first point in the tracing process of the rail guide's shape. The process is repeated for the entire range of motion of the knee, and set of base link angle configurations and the corresponding x-y directional deviations can be computed, as shown in (6).

$$\theta_i : \delta x_i, \delta y_i \tag{6}$$

Using the set of configurations of the base link angle and the corresponding x-y directional adjustments, as shown in (6), the required shape of the rail guide can be obtained, which ensures joint alignment of the SSLM's center of rotation in all three axes.

IV. Methods

A. 3D Trajectory Tracking of the Thigh and the Shin

The natural trajectory of the knee was recorded using a calibrated camera and ArUco markers [22], as depicted in Fig. 8. These markers were affixed to both the thigh and shin harness regions. The shin underwent movement from a fully extended position to full knee flexion. The orientation of the thigh was determined from the pose of the ArUco markers, while the orientation of the shin was estimated using a line passing through the markers located on the shin.

A coordinate transformation was performed to project the thigh onto the Transverse plane, enabling observation of the shin's motion relative to the thigh. Analysis was conducted on the discrete, frame-by-frame motion during knee flexion; however, this tracking method exhibited inaccuracies. Particularly, for flexion angles exceeding 90 degrees, the method demonstrated errors exceeding 1 cm. Given that approximately 70% of the recorded data fell within a 1 cm accuracy range, trajectory data for knee flexion angles under 90 degrees was included to assess the feasibility of the proposed 3D joint alignment concept.

B. Design Parameters for SSLM Links

The shin's 3D motion trajectory was used to construct the best-fit sphere that whose surface contained the most measured data points as shown in Fig. 9. The fitting algorithm calculates the center and the radius of the sphere that best

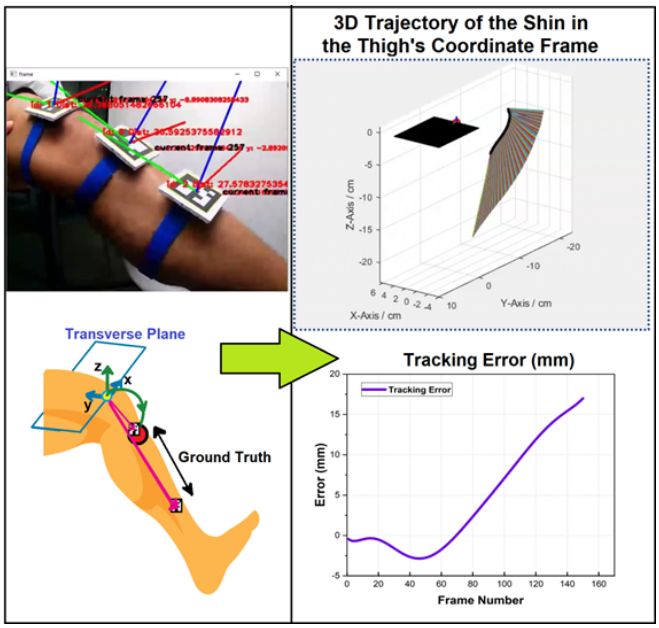

Fig. 8: Tracking the 3D trajectory of the knee. The thigh is situated in the Transverse plane and the shin's motion is observed. Because of notable tracking inaccuracies observed for flexion angles exceeding 90 degrees, only data for flexion angles below 90 degrees is utilized, to asses the feasibility.

represents the obtained shin trajectory points. The sphere was used to determine the knee's flexion angle at individual data points. The radius r of the best-fit sphere was 8.04cm, which was used to design the SSLM link's bending angle using (2). The patella width was used to determine l, and the number of links was determined based on the length of the patella and the minimum thickness required for structural rigidity under a 600N axial stress. Stress analysis indicated that Aluminum alloy could withstand this axial force without significant deformation, leading to its selection for manufacturing the joint.

Additionally, a suitable bearing-based rail-following mechanism was devised at the SSLM base link tips, along with a yaw constraint at the base joint. Bearing-based tendon routing was implemented on the links to separate the rotational motion of the links from interfering with the routes of tendon actuation. The finalized joint configuration is depicted in Fig. 4.

V. Evaluation

A. Joint Misalignment Experiment

To assess joint misalignment with the proposed knee joint, a pressure-based approach was utilized [16]. Pressure pads connected to small air pouches were positioned under the shin harness to detect undesired pressure buildup, indicative of misalignment. Additionally, for comparison purposes, a commercial knee-support brace with a single degree-of-freedom revolute joint was worn, and pressure pads were similarly placed for conducting the tests. The experimental setup is depicted in Fig. 10, where a knee flexion motion was executed. The shin actively displaced a rotary encoder to estimate the knee's flexion angle. Monitoring pressure variations facilitated the assessment of joint misalignment, as any pressure buildup could be directly attributed to misalignment between the knee and the exoskeleton.

In Fig. 11, the proposed joint mechanism shows significantly reduced pressure levels across all flexion angles compared to the conventional single DOF revolute joint. As the flexion angle increases, a corresponding increase in misalignment is observed, which remains lower than that of the single DOF commercial knee brace. It's important to note that due to tracking inaccuracies in knee trajectory data, as shown in Fig. 8, data for flexion angles only up to 90 degrees was included. The slight increase in pressure towards the end can also be attributed to tracking inaccuracies, which affect the shape of the guide rail, particularly at higher flexion angles. Thus, improving motion-tracking accuracy can help to create a more accurate guide rail shape, and further reduce the slight misalignment that is observed. Additionally, further alignment improvements can be achieved by addressing the

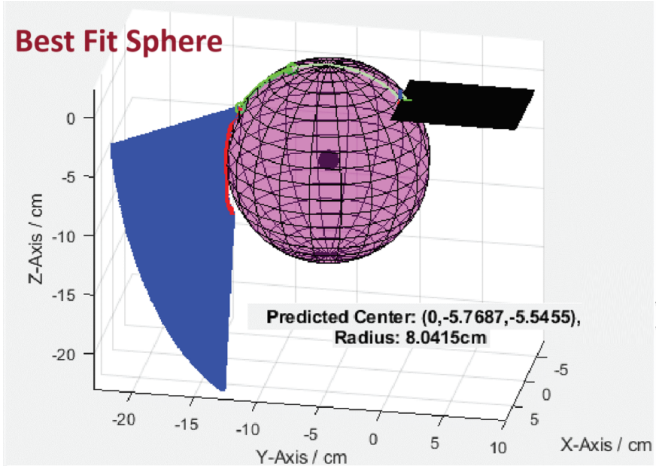

Fig. 9: Fitting the shin's 3D trajectory to the optimal sized-sphere which spans across the SSLM's workspace. The black plane represents the stationary thigh and the blue region represents the shin's motion.

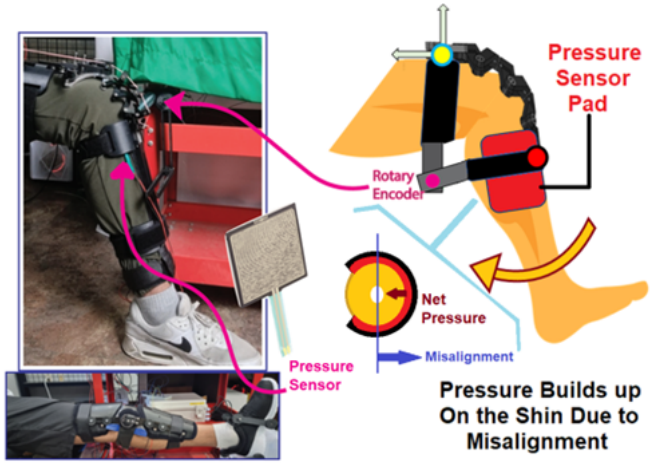

Fig. 10: Experimental setup for knee joint misalignment evaluation. The flexion angle was measured using a rotary encoder, while a thin, pressure-sensing pad was placed between the shin and the harness, to monitor the pressure buildup from joint misalignment.

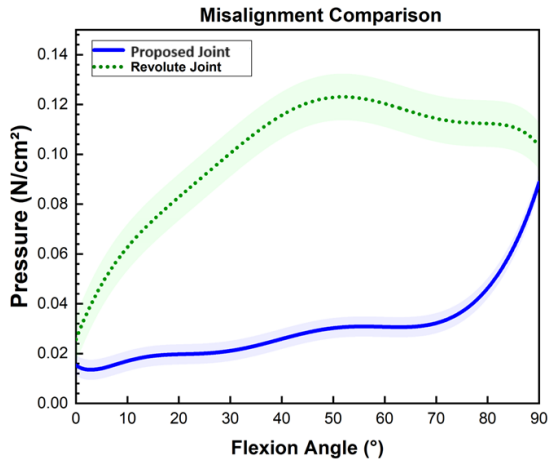

Fig. 11: Pressure data plot against knee flexion angle. Pressure buildup due to misalignment is significantly reduced. Towards a higher flexion angle, misalignment is seen to increase, which is attributed to the increasing motion tracking error of the shin. The results support the feasibility of the proposed joint.

small gliding motion of the knee, which was not considered in this study. Nevertheless, the significant reduction in misalignment demonstrates the feasibility of the proposed joint design.

B. Axial Rigidity Experiment

To validate the enhanced knee joint alignment was not attributed to the structural softness of the individual links in the Spherical Scissor Linkage Mechanism (SSLM). An experimental setup was designed, to verify that the SSLM has sufficient axial rigidity to support axial force. Sufficient axial rigidity implies that the moment arm of the SSLM is maintained even under the application of substantial axial force, as shown in Fig. 12. A tendon-based actuator called

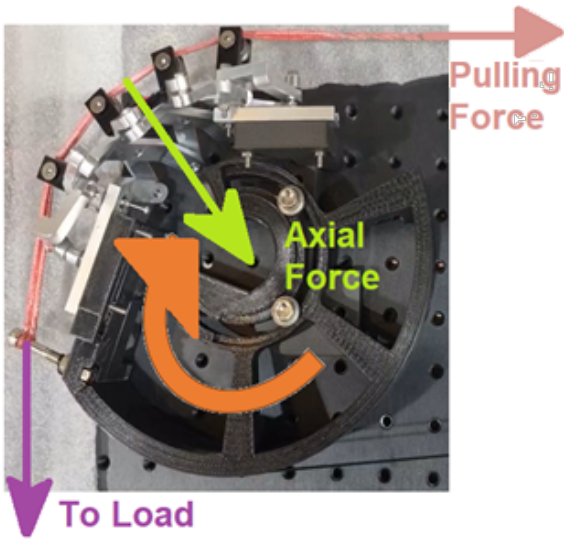

Fig. 12: Experimental setup to verify the SSLM's axial rigidity to maintain moment arm. A string actuator actuated a 15KG load over the SSLM, and the motor torque generated was measured from the motor driver's current.

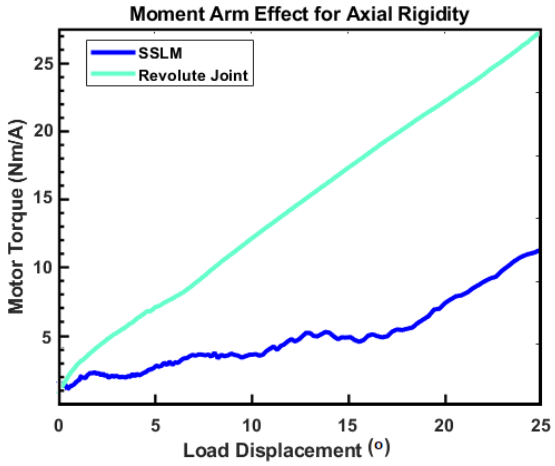

Fig. 13: The motor torque required to displace a given load is shown. The torque required was lowered due to the SSLM's moment arm, which verifies its axial rigidity property.

the Twisted String Actuator was guided over the SSLM, to lift a 15KG load. The same experiment was repeated with a revolute joint with a slightly, smaller moment arm. We monitored the force needed by the motor to complete the same task, from the Current measurements of the motor driver.

The plot in Fig. 13 showed a significant reduction in the motor torque that was required when the SSLM was used. This is attributed to the SSLM maintaining its moment arm, by supporting high axial force that was applied. Also, no visible deformation or collapse was noticed for the SSLM. Thus, the rigidity and axial support capability of the mechanism were verified, to prove the hybrid-stiffness nature of the proposed joint.

VI. Conclusion and Future Works

This work introduces a novel knee-joint exoskeleton designed to reduce joint misalignment by aligning with the knee's natural direction of motion in both the Sagittal and Coronal planes, while maintaining axial rigidity. This alignment was achieved using the Spherical Scissor Linkage Mechanism (SSLM) together with a rigid guide rail, used for adjusting the center of rotation of the SSLM with the knee's center of rotation. To the best of the author's knowledge, this is the first time knee joint alignment has been achieved across all three axes without relying on structurally soft materials. The hybrid-stiffness nature of the exoskeleton was experimentally verified, demonstrating inherent axial rigidity while maintaining knee-joint adaptability, all without the use of soft materials. It is important to note that the proposed joint requires customization to fit the user's knee properly. Future publications will address a more general approach to achieve automatic joint alignment.

References

[1] P. A. Costigan, K. J. Deluzio, and U. P. Wyss, "Knee and hip kinetics during normal stair climbing," *Gait & posture*, vol. 16, no. 1, pp. 31–37, 2002.

[2] E. A. Hurley, "Use of kafos for patients with cerebral vascular accident, traumatic brain injury, and spinal cord injury," *JPO: Journal of Prosthetics and Orthotics*, vol. 18, no. 7, pp. P199–P201, 2006.
[3] B. Chen, B. Zi, Z. Wang, L. Qin, and W.-H. Liao, "Knee exoskeletons for gait rehabilitation and human performance augmentation: A state-of-the-art," *Mechanism and Machine Theory*, vol. 134, pp. 499–511, 2019.
[4] M. Cenciarini and A. M. Dollar, "Biomechanical considerations in the design of lower limb exoskeletons," in *2011 IEEE International conference on rehabilitation robotics*. IEEE, 2011, pp. 1–6.
[5] W. Huo, S. Mohammed, J. C. Moreno, and Y. Amirat, "Lower limb wearable robots for assistance and rehabilitation: A state of the art," *IEEE systems Journal*, vol. 10, no. 3, pp. 1068–1081, 2014.
[6] D. Zanotto, Y. Akiyama, P. Stegall, and S. K. Agrawal, "Knee joint misalignment in exoskeletons for the lower extremities: Effects on user's gait," *IEEE Transactions on Robotics*, vol. 31, no. 4, pp. 978–987, 2015.
[7] A. MajidiRad, Y. Yihun, N. Hakansson, and A. Mitchell, "The effect of lower limb exoskeleton alignment on knee rehabilitation efficacy," in *Healthcare*, vol. 10, no. 7. MDPI, 2022, p. 1291.
[8] S.-S. Seo, *A Strategic Approach to Knee Arthritis Treatment: From Non-Pharmacologic Management to Surgery*. Springer, 2021.
[9] J. Hamill and K. M. Knutzen, *Biomechanical basis of human movement*. Lippincott Williams & Wilkins, 2006.
[10] A. M. Hollister, S. Jatana, A. K. Singh, W. W. Sullivan, and A. G. Lupichuk, "The axes of rotation of the knee," *Clinical Orthopaedics and Related Research®*, vol. 290, pp. 259–268, 1993.
[11] D. L. Churchill, S. J. Incavo, C. C. Johnson, and B. D. Beynnon, "The transepicondylar axis approximates the optimal flexion axis of the knee," *Clinical Orthopaedics and Related Research®*, vol. 356, pp. 111–118, 1998.
[12] M. K. Shepherd and E. J. Rouse, "Design and validation of a torque-controllable knee exoskeleton for sit-to-stand assistance," *IEEE/ASME Transactions on Mechatronics*, vol. 22, no. 4, pp. 1695–1704, 2017.
[13] J. Song, A. Zhu, Y. Tu, X. Zhang, and G. Cao, "Novel design and control of a crank-slider series elastic actuated knee exoskeleton for compliant human–robot interaction," *IEEE/ASME Transactions on Mechatronics*, vol. 28, no. 1, pp. 531–542, 2022.
[14] C. Ben-David, B. Ostraich, and R. Riemer, "Passive knee exoskeleton increases vertical jump height," *IEEE Transactions on Neural Systems and Rehabilitation Engineering*, vol. 30, pp. 1796–1805, 2022.
[15] B. Choi, Y. Lee, Y.-J. Kim, J. Lee, M. Lee, S.-g. Roh, Y. J. Park, K. Kim, and Y. Shim, "Development of adjustable knee joint for walking assistance devices," in *2017 IEEE/RSJ International Conference on Intelligent Robots and Systems (IROS)*. IEEE, 2017, pp. 1790–1797.
[16] T. Kim, M. Jeong, and K. Kong, "Bioinspired knee joint of a lower-limb exoskeleton for misalignment reduction," *IEEE/ASME Transactions on Mechatronics*, vol. 27, no. 3, pp. 1223–1232, 2021.
[17] C. Dai, P. Fu, B. Zhong, K. Guo, and M. Zhang, "Human-exoskeleton misalignment reduction on knee joint via an rpr mechanism-based device," in *2022 International Conference on Advanced Robotics and Mechatronics (ICARM)*. IEEE, 2022, pp. 45–50.
[18] C. Di Natali, T. Poliero, M. Sposito, E. Graf, C. Bauer, C. Pauli, E. Bottenberg, A. De Eyto, L. O'Sullivan, A. F. Hidalgo *et al.*, "Design and evaluation of a soft assistive lower limb exoskeleton," *Robotica*, vol. 37, no. 12, pp. 2014–2034, 2019.
[19] C. Chen, Y. Zhang, Y. Li, Z. Wang, Y. Liu, W. Cao, and X. Wu, "Iterative learning control for a soft exoskeleton with hip and knee joint assistance," *Sensors*, vol. 20, no. 15, p. 4333, 2020.
[20] J. Kim, T. Kim, C. Ko, S. Lee, and K. Kong, "Bio-inspired cable-driven knee orthosis for tibiofemoral joint load distribution," *IFAC-PapersOnLine*, vol. 55, no. 27, pp. 430–435, 2022.
[21] M. N. Castro, J. Rasmussen, M. S. Andersen, and S. Bai, "A compact 3-dof shoulder mechanism constructed with scissors linkages for exoskeleton applications," *Mechanism and Machine Theory*, vol. 132, pp. 264–278, 2019.
[22] S. Garrido-Jurado, R. Muñoz-Salinas, F. J. Madrid-Cuevas, and M. J. Marín-Jiménez, "Automatic generation and detection of highly reliable fiducial markers under occlusion," *Pattern Recognition*, vol. 47, no. 6, pp. 2280–2292, 2014.